Multi Directional Piezoelectric Plate Energy Harvesters Designed By Topology Optimization Algorithm

Abbas HOMAYOUNI-AMLASHI[1], Abdenbi MOHAND-OUSAID[1] and Micky RAKOTONDRABE[2], *member, IEEE*

***Abstract*—In this paper, piezoelectric plate energy harvesters are designed by using topology optimization algorithm to harvest the excitation from different directions. The goal is to minimize the volume and weight of the whole structure so the harvesters can be used in small scale applications. To this aim, the profile of polarization is optimized by the topology optimization to overcome charge cancellation which is the main challenge in random direction excitation. Two optimized designs with uniform and non-uniform polarization profiles are obtained. Separated electrodes in the surfaces of the optimized design with non-uniform polarization are used to simulate the polarization profile. Numerical simulations by COMSOL multi-physics software show that the optimized design with separated electrodes can provide 3 times higher voltage and power than those obtained with non-optimized piezoelectric plate. Experimental investigation demonstrated that the same design with separated electrodes can have 2.17 and 1.93 times higher voltage than the full plate for out of plane and in-plane forces respectively.**

***Index Terms*—Product Design, Development and Prototyping, Piezoelectric Energy Harvesting, Topology Optimization**

I. INTRODUCTION

ENERgy harvesters based on mechanical vibration are well known and their applications are well established [1]. By converting vibration energy to electrical energy, such systems offer a potential alternative to batteries in low-power-wireless devices such as wearable clothes [2], wireless sensors [3], GPS tracking systems [4] and small scale robots [5]. Piezoelectric effect is one of the main principles that allows such mechanical to electrical conversion, in particular at small scales [6], [7]. Among the different types of configurations for Piezoelectric Energy Harvesters (PEHs), cantilevered structures are widely used. In fact for a given input force, they provide the highest average strain energy [8], are easier to fabricate and appropriate for small scales applications. As such, for improving the harvested energy by cantilever PEHs, various methods have been proposed: parametric optimization [9], layers number optimization [10]. It is worth to note that interval techniques [11] are also potential parametric optimization for piezoelectric structures as demonstrated in [12].

In addition to the above optimization of PEHs, another promising optimization method that attracted the attention of researchers in order to improve their performances is the so-called Topology Optimization (TO). TO methodology is about integrating the Finite Element Method (FEM) with the optimization method [13]. The goal is to distribute in an optimal way the material within the design domain in order to have the best structural performance. One of the famous approaches of TO is the density approach [14] or more particularly the SIMP approach [15] which represents the Solid Isotropic Material with Penalization. In this approach, the optimization algorithm lets the elements in the design domain have an artificial density between zero and one multiplied by the material density. Due to the triumph of this approach, the implementation MATLAB code is also published with 3D FEM modelling [16]. This methodology was interesting enough to be applied to piezoelectric structures. As such, after taking the first step of extending the SIMP scheme for the non-isotropic material [17], the application of TO to piezoelectric materials took different directions including the optimization of actuators [18], sensors [19] and energy harvesters [20], [21]. The application of TO to PEHs started by defining an energy-based objective function and sensitivity analysis [20]. Thereafter, other works optimized the PEHs for dynamic forces [22] while recent works are considering the coupled electrical circuit in the optimization algorithm [23]. However, most of the research which integrated the TO to PEHs are theoretical and experimental investigations are difficult to be found in this field to the knowledge of authors. Moreover, the current status of research in PEHs area is that these latter configurations are mostly one degree of freedom, i.e. they only harvest the energy from one direction of excitation. The general approach for multi directional energy harvesters which is proposed recently is to attach the piezoelectric material to a passive structure which can vibrate in multi direction [24]. In this case however, the obtained structure will have higher volume and weight. As a summary, multi directional PEHs are extremely challenging for small scales applications if one should consider dimensions constrain, fabrication difficulty and possibly cost issues.

The aim of this paper is to exploit TO methodology in

Manuscript received: September, 10, 2019; Revised November, 29, 2019; Accepted December, 16, 2019.

This paper was recommended for publication by Editor Youngjin Choi upon evaluation of the Associate Editor and Reviewers' comments. *This work has been supported by the national CODE-TRACK project (ANR-17-CE05-0014-01, Control theory tools for optimal design of piezoelectric energy harvesters devoted to birds tracking devices). This work has also been partially supported by the Bourgogne Franche-Comté region project COMPACT.

[1] First Author and Second Author are with Department Automatique et Systèmes Micro-Mécatroniques, FEMTO-ST Institute, Université Bourgogne Franche-Comté, CNRS, Besançon 25000, France. (abbas.homayouni@femto-st.fr;abdenbi.mohand@femto-st.fr)

[2] Third Author is with Laboratoire Génie de Production, National School of Engineering in Tarbes (ENIT), INP University of Toulouse, France. (mrakoton@enit.fr)

Digital Object Identifier (DOI): see top of this page.

order to optimize PEHs structures that can harvest the energy from different directions of vibration excitation where there is a constraint on the weight and volume. The possible application includes miniaturized wireless sensors and tracking devices with lowest possible amount of cost and complexity of fabrication. The initial design domain is a square piezoelectric plate. A mechanical boundary condition is suggested instead of conventional cantilever beam that can make the harvested energy from different directions as much symmetric as possible. The TO code written by the authors is the active piezoelectric material extension of the 3D MATLAB code published in [16] which was written for classical passive structures. Considering the application of multiple forces which represent the random directional force, the main challenge is the charge cancellation that can happen within the obtained design. To remedy this, polarization optimization is also considered in the TO algorithm via the method of PEMAP-P [18]. The electrodes are separated based on the obtained polarization profile which is a cheap process in terms of cost and complexity of fabrication. The proposed objective function can reduce the numerical instabilities and the effects of choosing different optimization parameters on the final design. Furthermore, to avoid the numerical instabilities due to huge scale difference between piezoelectric matrices a normalization is suggested as well.

Two different optimized designs are obtained by considering two different possible of applied force configuration. The performance of these two optimized designs under different excitation forces is investigated numerically via finite element (FE) method by COMSOL Multiphysics (COMSOL, Inc.,Burlington, USA) simulation and then experimentally. The experimented optimized structures were fabricated with piezoelectric bi-morph plates and laser cutting machine. The excitation during the experimental tests was done by attaching a magnet at the extremity of each PEH and applying a magnetic field to them thanks to a controlled electromagnet. Numerical and experimental results demonstrated two times better performance from the optimized design with separated electrodes in comparison with the simple full plate design. Moreover, the obtained designs here are scalable i.e. the suggested boundary condition, the obtained optimized designs, the proposed method to avoid the charge cancellation and the fabrication process can be easily implemented in small and micro dimension applications.

II. Piezoelectric Finite Element Modelling

In Fig. 1(a) the schematic view of a bi-morph piezoelectric plate (PZTP) with defined clamped boundary condition, attached mass and forces in 3 directions are illustrated. The bi-morph plate consists of 3 electrodes: on top, middle and bottom surfaces of the plate. The polarization axes for the piezoelectric materials is parallel to the z direction of the coordinate system while the direction will be later defined by optimization method. This following initial design is proposed here to harvest the vibrational energy that comes from different directions. The FE modelling of the system is started by discretizing the design domain by finite number of 3D hexahedron elements as shown in Fig. 1(b). Each element has 8 nodes and each node has 3 mechanical degrees of freedom as displacement [25] and one electrical degree of freedom as potential [26]. By using enough number of 3D elements, the FEM model will be accurate. Starting from piezoelectric constitutive equations and by (i) neglecting the thermal coupling and damping effects, (ii) performing the mathematical procedure given in [26], the following finite element equation can be achieved

$$\begin{bmatrix} M & 0 \\ 0 & 0 \end{bmatrix} \begin{bmatrix} \ddot{U} \\ \ddot{\Phi} \end{bmatrix} + \begin{bmatrix} K_{uu} & K_{u\phi} \\ K_{\phi u} & -K_{\phi\phi} \end{bmatrix} \begin{bmatrix} U \\ \Phi \end{bmatrix} = \begin{bmatrix} F \\ Q \end{bmatrix} \tag{1}$$

where U and ϕ are the vectors of the mechanical displacement and electric potential respectively. F and Q are the applied external mechanical force and electrical charge. M, K_{uu}, $K_{u\phi}$, $K_{\phi\phi}$ are the global mass matrix, mechanical stiffness matrix, piezoelectric coupling matrix and piezoelectric permittivity matrix respectively. These matrices are formed by assembling the elemental matrices [22].

For the energy harvesting case, first, the applied external charge (Q) in (1) is considered to be zero. Then, by considering a harmonic external force and assuming a linear electromechanical system, the force and the response of the system will be modelled in the following form

$$F = F_0 e^{i\Omega t}, U = U_0 e^{i\Omega t} \tag{2}$$

where Ω is the excitation frequency. As such, the equilibrium equation in (1) can be rewritten as

$$\begin{bmatrix} K_{uu} - M\Omega^2 & K_{u\phi} \\ K_{\phi u} & -K_{\phi\phi} \end{bmatrix} \begin{bmatrix} U \\ \Phi \end{bmatrix} = \begin{bmatrix} F \\ 0 \end{bmatrix} \tag{3}$$

The new equation in (3) can't be solved due to singularity. General approach to deal with this issue is to apply mechanical and electrical boundary conditions. However, in addition to singularity, the huge scale difference of the internal matrices including stiffness matrix and permittivity matrix brings numerical instability in computational procedures. Therefore, here it is proposed to perform a normalization which starts from the elemental matrices as follows

$$\tilde{K}_{uu} = \frac{1}{k_0}\sum_{i=1}^{NE} k_{uu}, \tilde{K}_{u\phi} = \frac{1}{\alpha_0}\sum_{i=1}^{NE} k_{u\phi}$$
$$\tilde{K}_{\phi\phi} = \frac{1}{\beta_0}\sum_{i=1}^{NE} k_{\phi\phi}, \tilde{M} = \frac{1}{m_0}(\sum_{i=1}^{NE} m + [M_{mass}]) \tag{4}$$

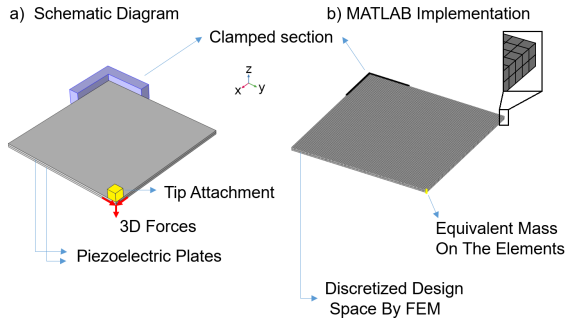

Fig. 1. Piezoelectric plate energy harvester modelling. a) Schematic modelling of piezoelectric plate under application of 3 directional force b) finite element modelling in MATLAB environment

where m, k_{uu}, $k_{u\phi}$, $k_{\phi\phi}$ are the elemental matrices and global mass matrices are formed by assembling these elemental matrices while factorizing the biggest value of each matrix elements which are k_0, α_0, β_0 and m_0. ($\tilde{}$) shows the normalized matrices. To model the attached mass, its equivalent mass is modelled as a lumped mass on the desired elements. This assumption is accurate since the mass of the tip attachment is several times less than the mass of the piezoelectric plate. Now, with the aforementioned normalization, the equilibrium equation (3) can be rewritten in the following form

$$\begin{bmatrix} \tilde{K}_{uu} - \tilde{M}\tilde{\Omega}^2 & \tilde{K}_{u\phi} \\ \tilde{K}_{\phi u} & -\gamma\tilde{K}_{\phi\phi} \end{bmatrix} \begin{bmatrix} \tilde{U} \\ \tilde{\Phi} \end{bmatrix} = \begin{bmatrix} \tilde{F} \\ 0 \end{bmatrix} \tag{5}$$

where

$$\begin{gathered} \tilde{F} = F/f_0, \tilde{U} = U/U_0, , \tilde{\Phi} = \Phi/\Phi_0 \\ U_0 = f_0/k_0, \Phi_0 = f_0/\alpha_0 \\ \tilde{\Omega}^2 = m_0\Omega^2/k_0, \gamma = k_0\beta_0/\alpha_0^2 \end{gathered} \tag{6}$$

In (5), f_0 is the amplitude of the force and the variables U_0 and Φ_0 are the normalization factors of the displacement and potential which are function of other normalization factors. The variable γ is having the scale of 10^1 and it guarantees that the solution of the system will remain the same before and after applying the normalization. With eliminating the scale difference between the matrices, the numerical instability is highly decreased. To apply the mechanical boundary condition, the clamped part of the piezoelectric plate in Fig. 1(a) is modelled by forcing zero displacement to the nodes which are illustrated in Fig. 1(b). To apply the electrical boundary condition for the bi-morph piezoelectric plate, the middle electrode is modelled as ground to have zero potential. Equipotential condition for the nodes attached to the electrodes can be written as [22]

$$\tilde{\Phi} = BV_p \tag{7}$$

in which, B is a Boolean matrix with dimension $N_e \times N_P$ where N_e is the number of nodes and N_P is the number of electrodes. Now, after applying the mechanical and boundary conditions, the final form of the equilibrium equation can be written as

$$\begin{bmatrix} \overline{K_{uu}} & \overline{K_{u\phi}} \\ \overline{K_{\phi u}} & -\overline{K_{\phi\phi}} \end{bmatrix} \begin{bmatrix} U \\ V_p \end{bmatrix} = \begin{bmatrix} F \\ 0 \end{bmatrix} \tag{8}$$

in which

$$\begin{gathered} \overline{K_{uu}} = \left[\tilde{K}_{uu} - \tilde{M}\tilde{\Omega}^2\right]_{bc}, \overline{K_{u\phi}} = \left[\tilde{K}_{u\phi}B\right]_{bc} \\ \overline{K_{\phi\phi}} = \gamma B^T\tilde{K}_{\phi\phi}B \end{gathered} \tag{9}$$

where ($[\ ]_{bc}$) shows the application of mechanical boundary condition. It should be noted that one element per thickness of the PZTP layer is chosen. This is accurate enough since the ratio of thickness to length for each PZTP layer is considered to be around 0.01. Now, based on the built FEM model of the piezoelectric plate, topology optimization algorithm can be applied .

III. Topology Optimization

A. Problem Formulation

Generally, the objective function for the topology optimization of the piezoelectric energy harvesters is considered to be the ratio of the electrical energy to the mechanical energy [20], [22] or the electromechanical coupling coefficient [27]. However due to numerical instability that can be caused by defining these objective functions, some recent researches proposed to penalize the mechanical energy [23], [27]. In addition to numerical instability, by considering the objective function as energy ratio, penalization factors changes the results of the optimization extremely as reported by Noh et al. [22]. Since there is no information on how to choose the penalization factors, finding the optimal structure is a cumbersome trial and error approach for choosing different combinations of penalization factors while still the final result can have no physical meaning, i.e. it is not possible to produce the design due to discontinuity or mechanical instability. To tackle the aforementioned challenges, here the difference between mechanical and electrical energy multiplied by a weighting factor is considered as objective function. Therefore, the optimization problem can be defined as

$$\begin{gathered} Minimize \quad J = w_j\Pi^S - (1-w_j)\Pi^E \\ Subject\ to \quad V(x) = \sum_{i=1}^{NE} x_i v_i \le V, \\ 0 \le x_i \le 1, 0 \le P_i \le 1 \end{gathered} \tag{10}$$

In which, J is the objective function, w_j is the weighting factor, x_i and P_i are design variables that present the density ratio and polarization of each element respectively. (V) is the target volume which is a fraction of the overall volume of the design domain while v_i is the volume of each element and NE is the total number of elements. Π^S and Π^E are mechanical and electrical energies respectively which are defined in the following form [22], [20]

$$\Pi^S = (\frac{1}{2})\tilde{U}^T\overline{K_{uu}}\tilde{U}, \Pi^E = (\frac{1}{2})V_p^T\overline{K_{\phi\phi}}V_p \tag{11}$$

In (10), w_j determines the importance of each energy during the optimization. It is obvious that if $w_j = 1$ then the optimization will be the minimization of the mean compliance [16], [13]. With reducing the w_j the optimization will shift towards maximization of the electrical energy. But, it should be noted that very low values for the w_j may lead to mechanically unstable results.

B. Sensitivity Analysis

Gradient based optimization requires the sensitivity of objective function with respect to each design variable. Here, the design variables are density ratio and polarization. For density, the derivative of objective functions is calculated in the following form

$$\frac{\partial J}{\partial x_i} = w_j\frac{\partial\Pi^S}{\partial x_i} - (1-w_j)\frac{\partial\Pi^E}{\partial x_i} \tag{12}$$

Now, by substituting (11) to (12) the similar procedure explained in ref [20] can be followed to calculate the sensitivities.

However, the normalization factor (γ) is introduced to the formulation here

$$\frac{\partial \Pi^S}{\partial x_i} = (\frac{1}{2}\tilde{u}_i^T + \lambda_{1,i}^T)\frac{\partial(\tilde{k}_{uu} - \tilde{m}\tilde{\Omega}^2)}{\partial x_i}\tilde{u}_i + \lambda_1^T \frac{\partial \tilde{k}_{u\phi}}{\partial x_i}\tilde{\phi}_i + \mu_{1,i}^T \frac{\partial \tilde{k}_{\phi u}}{\partial x_i}\tilde{u}_i - \mu_{1,i}^T \frac{\gamma \partial \tilde{k}_{\phi\phi}}{\partial x_i}\tilde{\phi}_i \quad (13)$$

$$\frac{\partial \Pi^E}{\partial x_i} = \frac{1}{2}\tilde{\phi}_i^T \frac{\partial \tilde{k}_{\phi u}}{\partial x_i}\tilde{\phi}_i - \mu_{2,i}^T \frac{\gamma \partial \tilde{k}_{\phi\phi}}{\partial x_i}\tilde{\phi}_i + \lambda_{2,i}^T \frac{\partial(\tilde{k}_{uu} - \tilde{m}\tilde{\Omega}^2)}{\partial x_i}u_i + \lambda_2^T \frac{\partial \tilde{k}_{u\phi}}{\partial x_i}\tilde{\phi}_i + \mu_2^T \frac{\partial \tilde{k}_{\phi u}}{\partial x_i}\tilde{u}_i \quad (14)$$

In (13) and (14) which are the sensitivity of mechanical and electrical energy respectively, μ and λ are the elemental adjoint vectors to avoid taking the derivative of u and ϕ with respect to design variables. These adjoint vectors are calculated by the following global coupled system

$$\begin{bmatrix} \overline{K_{uu}} & \overline{K_{u\phi}} \\ \overline{K_{\phi u}} & -\overline{K_{\phi\phi}} \end{bmatrix} \begin{bmatrix} \Lambda_1 \\ \Upsilon_1 \end{bmatrix} = \begin{bmatrix} -\overline{K_{uu}}U \\ 0 \end{bmatrix} \quad (15)$$

$$\begin{bmatrix} \overline{K_{uu}} & \overline{K_{u\phi}} \\ \overline{K_{\phi u}} & -\overline{K_{\phi\phi}} \end{bmatrix} \begin{bmatrix} \Lambda_2 \\ \Upsilon_2 \end{bmatrix} = \begin{bmatrix} 0 \\ -\overline{K_{\phi\phi}}V_p \end{bmatrix} \quad (16)$$

where Λ and Υ, are the global adjoint vectors which need to be disassembled to form the elemental adjoint vectors

$$[\lambda_1]_{bc} = \Lambda_1, [\lambda_2]_{bc} = \Lambda_2, [\mu_1] = B\Upsilon_1, [\mu_2] = B\Upsilon_2 \quad (17)$$

It is worthwhile to mention that, solving equations (8), (15) and (16) with applied equipotential condition reduces the size of the system significantly which boosts the speed of calculations in each iteration of optimization. To calculate the derivatives of the stiffness matrix, piezoelectric coupling matrix and piezoelectric permittivity, the SIMP scheme for isotropic material can be extended to the piezoelectric material which will be discussed next.

C. Extension of SIMP Scheme to Piezoelectric Material

In case of SIMP scheme, the Young module of elasticity of each element equals to the multiplication of the element density ratio (x) and the Young module of the isotropic material. [13]. However, for the non-isotropic piezoelectric material, the density ratio will be multiplied to the whole stiffness and piezoelectric matrices. Therefore, the extension of SIMP to the piezoelectric materials can be written as [22], [18]

$$\begin{aligned} \tilde{k}_{uu}(x) &= x^{p_{uu}}\tilde{k}_{uu} \\ \tilde{k}_{u\phi}(x,P) &= x^{p_{u\phi}}(2P-1)^{p_P}\tilde{k}_{u\phi} \\ \tilde{k}_{\phi\phi}(x) &= x^{p_{\phi\phi}}\tilde{k}_{\phi\phi} \\ \tilde{m}(x) &= x\tilde{m} \end{aligned} \quad (18)$$

where, p_{uu}, $p_{u\phi}$ and $p_{\phi\phi}$ are the stiffness, coupling and permittivity penalization coefficients. Coupling Matrix $\tilde{k}_{u\phi}(x,P)$ is a function of density (x) and polarization (P) which is penalized by factor p_P. This methodology which introduces the polarization as a variable in the optimization is known as "piezoelectric material with penalization and polarization" (PEMAP-P) [18] and defines the direction of polarization for each element during optimization. Different values can be considered for penalization factors. It is already known that the stiffness penalization factor p_{uu} should be more than 3 [13]. For other penalization coefficients, Noh et al. [22] considered different values for a cantilever under bending force and those results cannot be extended to the other design configuration like the one proposed in this paper. However, with objective function defined in (10), the effect of penalization factors on the optimization is minimized. The suggestion here is to use values greater than 3 for $p_{u\phi}$ and $p_{\phi\phi}$ and value of 1 for p_P since no penalization is needed for polarization. In fact, the values of $p_{u\phi}$ and $p_{\phi\phi}$ do not have any effect on the final topology. But, they steer the elements of the final topology to zero and one density (black and white design [13]) more effectively. Now, with the help of (18) it is possible to take the derivative of the piezoelectric matrices with respect to density ratio

$$\begin{aligned} \frac{\partial \tilde{k}_{uu}(x)}{\partial x} &= p_{uu}x^{p_{uu}-1}\tilde{k}_{uu} \\ \frac{\partial \tilde{k}_{u\phi}(x,P)}{\partial x} &= p_{u\phi}x^{p_{u\phi}-1}(2P-1)^{p_P}\tilde{k}_{u\phi} \\ \frac{\partial \tilde{k}_{\phi\phi}(x)}{\partial x} &= p_{\phi\phi}x^{p_{\phi\phi}-1}\tilde{k}_{\phi\phi} \\ \frac{\partial \tilde{m}(x)}{\partial x} &= \tilde{m} \end{aligned} \quad (19)$$

By Substituting (19) in (13) and (14), the sensitivity of objective function with respect to density ratio can be calculated. In addition to what is mentioned in refs [20], [22], by employing the PEMAP-P [18], polarization is also a variable of optimization. As such, here the sensitivity of objective function with respect to polarization is calculated as well

$$\frac{\partial \Pi^S}{\partial P_i} = \lambda_1^T \frac{\partial \tilde{k}_{u\phi}}{\partial P_i}\tilde{\phi}_i + \mu_{1,i}^T \frac{\partial \tilde{k}_{\phi u}}{\partial P_i}\tilde{u}_i \quad (20)$$

$$\frac{\partial \Pi^E}{\partial P_i} = \frac{1}{2}\tilde{\phi}_i^T \frac{\partial \tilde{k}_{\phi u}}{\partial P_i}\tilde{\phi}_i + \lambda_2^T \frac{\partial \tilde{k}_{u\phi}}{\partial P_i}\tilde{\phi}_i + \mu_2^T \frac{\partial \tilde{k}_{\phi u}}{\partial P_i}\tilde{u}_i \quad (21)$$

While the adjoint vectors μ and λ are already calculated through the coupled system defined in (15) and (16) and just the derivative of the piezoelectric coupling matrix with respect to polarization is needed. This derivative is given as follows

$$\frac{\partial \tilde{k}_{u\phi}(x,P)}{\partial P} = 2p_P(2P-1)^{p_P-1}x^{p_{u\phi}}\tilde{k}_{u\phi} \quad (22)$$

D. Updating Optimization Variables

After defining the optimization problem and performing the sensitivity analysis, Method of Moving Asymptotes (MMA) [28] is utilized to update the optimization variables while respecting the volume constraint. Here, the optimization variables are density ratio and polarization.

After updating the densities by MMA, density filter is applied to avoid the numerical instabilities like mesh-dependency and checkerboard patterns and the theoretical concept behind is explained in [13]. Here, to apply the density filter the same lines of codes proposed by Liu et al. [16] are employed.

E. Piezoelectric Topology Optimization Algorithm

The topology optimization algorithm for piezoelectric material can be written in the following form:

Initial guess for the x and P;
while *Density Change > 0.01 & loop number < Maximum loop* **do**
  Computing $\tilde{K}_{uu}$, $\tilde{K}_{u\phi}$, $\tilde{K}_{\phi\phi}$, $\tilde{M}$;
  Applying mechanical and electrical boundary conditions;
  Calculation of system responses U and V_P;
  Calculation of objective function J;
  Sensitivity analysis for x and P;
  Updating x and p using MMA;
  Application of density filter;
end
Post processing

In post processing step, the density ratios of the obtained design are firstly steered to 0 and 1. Then the coordinates of the boundaries are used to transfer the design to the CAD software. Here, the post processing method mentioned in [29] which consists of two steps of Gaussian filter and thresholding is employed.

IV. Numerical Results and Simulation

A. MATLAB FEM Topology Optimization Results

In this section the piezoelectric plate illustrated in Fig.1-(b) is optimized by the optimization algorithm regarding the force and boundary conditions. The specifications of the PZTP and optimization parameters are reported in table I. Here, the geometry of the design domain is chosen based on the available fabrication instruments. In fact, increasing or decreasing the scale of the design domain will not change the result of optimization. The excitation frequency is considered to be 20 Hz which is in the range of real applications like vehicle vibration and animal GPS tracking devices. The sensitivity of the objective function respect to applied frequency is low and the applied frequency should be changed considerably to have small effect on the final layout of the obtained results.

The results of the TO in MATLAB for two cases are shown in Fig. 2-(a) and (c) including the elements which have density ratio more than 0.9 while the red color of the elements shows the positive polarization in direction of z coordinate and the blue color shows opposite polarization.

The optimized design (1) is the result of optimization for forces in 3 directions and optimized design (2) is the result of optimization when there are just in-plane forces in directions of x and y and the force in direction of z is completely neglected. Since the produced electrical energy due to out of plane force i.e. z direction is highly superior to the in-plane forces, the optimization algorithm considers constant polarization in each layer when there is out of plane force, as can be seen in 2-(a). The problem of this polarization profile is that in case of planar force, there will be charge cancellation due to compression and tension in different parts of the layer. To remedy this, in the second approach, the goal is to just optimize the design for in-plane forces while it is known that the energy of out of plane forces are higher in several order. As it is obvious from Fig. 2-(c), the polarization profile in the second row design is not constant and direction of the polarization in different parts of the layer is changed to avoid charge cancellation. For the realization of this polarization profile, the top and bottom electrode as it is shown in Fig. 2-(d) are divided to two sections to simulate the polarization profile. As such, the design has two electrodes on top, two electrodes on bottom and one electrode in the middle. For practical reasons, this division of electrodes is not completely following the polarization profile. In fact, exact implementation of polarization profile makes the realization extremely complicated in terms of fabrication and electrical circuit.

TABLE I
Parameters

Parameter	Value	Parameter	Value
PZTP Type	PZT PSI-5H4E	Tip Magnet Weigth	50 (milligram)
PZTP density	7800 (kg/m^3)	p_{uu}	3
PZTP Thickness	0.254(mm)	$p_{u\phi}$	6
PZTP Length	19.1 (mm)	$p_{\phi\phi}$	6
PZTP Width	19.1 (mm)	p_P	1
FEM Number of Elements	$100 \times 100 \times 2$	Excitation Frequency	20 HZ
Clamping Fraction	0.3	Density Filter Radius	1.5
Volume Fraction	0.4	w_j	0.02

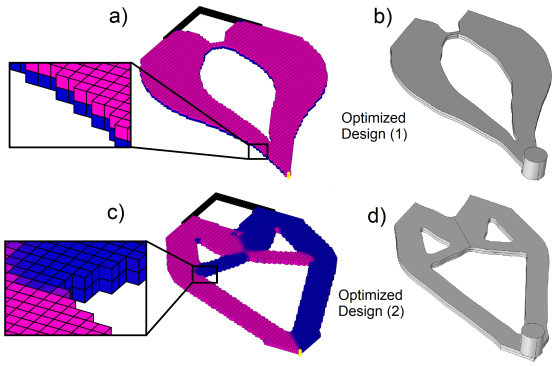

Fig. 2. Optimized designs obtained by topology optimization. (a) and (c): MATLAB FEM, (b) and (d): COMSOL implementation

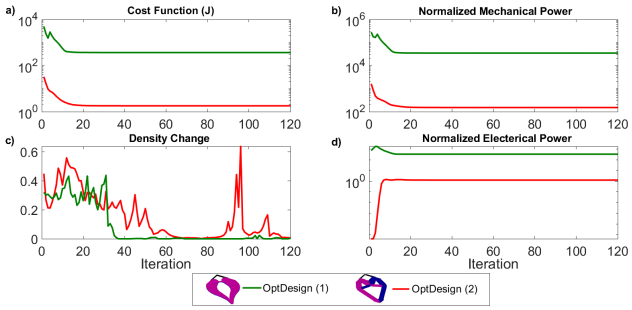

Fig. 3. MATLAB topology optimization implementation

The changes of mechanical and electrical power, density change and volume fraction during the TO iterations are illustrated in Fig. 3. It is obvious that mechanical and electrical power converge very smoothly without numerical instabilities. The optimization is stopped manually after 120 iterations since no significant change in powers or obtained design could be

seen. The reason that electrical and mechanical power for optimized design (1) is several order higher than the optimized design (2) is that for optimized design (2), there is no force in the z direction. Such force is a bending force and produces a large strain and significant mechanical and electrical energy.

B. COMSOL Simulation

After transferring the design to COMSOL multi-physics software, their responses due to a force in different directions are investigated. Mechanical boundary condition and electrodes are defined respectively. For each electrode an electrical circuit is modelled separately in the software to measure the voltage, the electrical and the mechanical power obtained from the design due to a harmonic force.

A general force in the 3D space with random directions can be decomposed to its perpendicular components along X, Y and Z axes. Since two of these components are parallel to X and Y axes, the performance of the optimized designs depends on how they can avoid in-plane charge cancellation. Therefor, in Fig.4, it is considered that an in-plane force is applied to the designs in different directions. Then the voltage, electric power, mechanical power and power ratio are reported to compare the performance of the designs. In Fig.4-(a), the representation of the applied force is shown. In fact, the amplitude of the force is constant. Only the angle α is changing from 0 to 2π with the steps of $\pi/12$. So Fig.4-(d), it is obvious that the amplitude of force is constant and just the angle of application force is changing while each point on the plot shows the steps of angle changes.

Now, in Fig.4-(b), the voltages related to all points are calculated as well. As such, the direction of each point to the center shows the direction of the force. But, the distance of each point to the center shows the voltage. In the remaining parts of the figure, i.e. mechanical power, electric power and power ratio, the direction of each point to the center shows the direction of the force but the distance shows the amplitude of the parameter. By inspecting the plots it is revealed that optimized designs (1) and (2) produce around up to 2 and 3 times higher output voltage and power in comparison with full plate respectively. The power ratio which is the ratio of the electrical power to mechanical power shows that the best power ratio still belongs to optimized design (2) while the optimized design (1) has lower electrical to mechanical power ratio. The reason for low power ratio for optimized design (1) due to in-pane force is the charge cancellation resulted by the uniform electrodes.

The maximum of piezoelectric voltage and power depend on amplitude and distribution of mechanical strain energy. For different direction of excitation force, there can be stress concentration nearby the clamping. This leads to the existence of a jump in the mechanical energy stored in the design while the distribution of strain is non-uniform. For this reason, the peaks of mechanical power and electrical power are not the same in Fig. 4.

In Fig. 5, to assess the performance of different design it is considered that the force can be applied at different directions in 3D space as shown in part Fig. 5-(a) To define

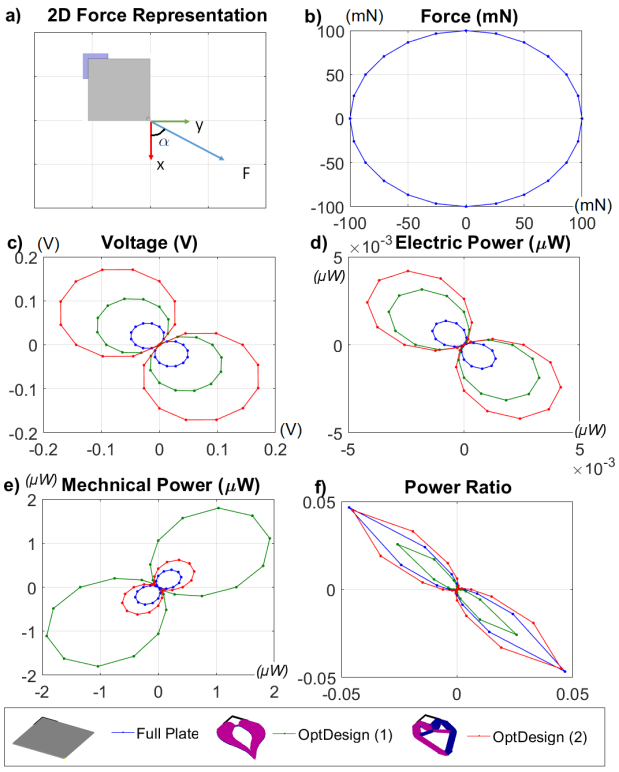

Fig. 4. COMSOL FEM results to investigate the performance of designs under application of 2D in-plane force

the direction of the force, two angles α and β are used. To discretize the continuous domain of direction that the force can have, the angle β is changing from 0 to $\pi/2$ with steps of $\pi/24$ and angle α is changing similarly to before, i.e. to Fig. 4. Again, like previous assessment for 2D forces, the direction of each point to the center is the direction of the applied force but the distance is the related parameter. The performance improvement of the optimized design (1) and (2) in comparison with full plate design is around 2 and 3 times. In contrast to in-plane force, the improvement in power ratio is more considerable especially for optimized design (1) which had a low power ratio for in-plane forces. However, the voltage and power of the optimized design (2) is higher. This is due to the fact that optimized design (2) can avoid the charge cancellation within the PZT layer thanks to separated electrodes.

It is obvious that the power and voltage for out of plane forces are higher than the ones for in-plane forces due to higher planar stiffness. Although, in real applications the applied force is less likely to be completely planar, to decrease the planar stiffness, it is possible to decrease the volume fraction. In this case, the design would be more fragile, however increasing the thickness can be suggested to reducing the possibility of fracture.

V. Experimental Investigation

A. Fabrication

The fabrication process of designs started by gluing two piezoelectric plates with a dimensions of 75x75x0.254 mm

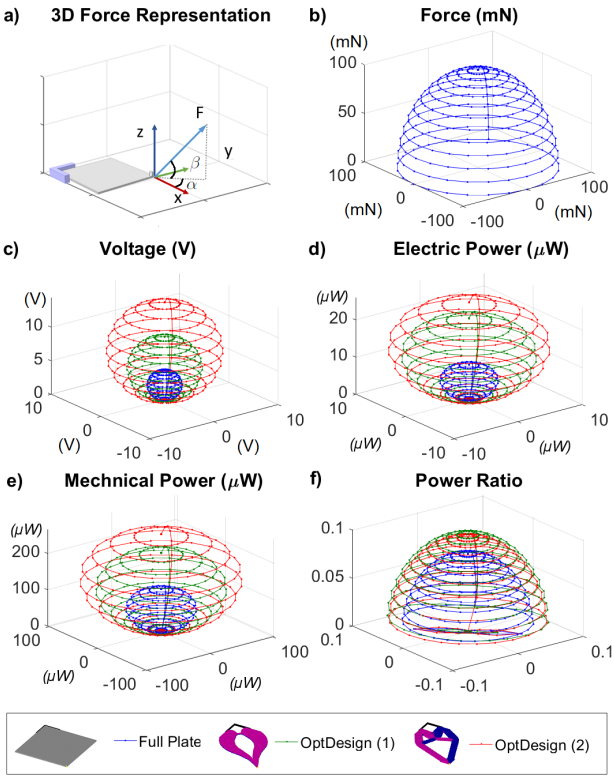

Fig. 5. COMSOL FEM results to investigate the performance of designs under application of 3D force

(commercial PZT - lead zirconate titanate - piezoelectric material PSI-5H4E from Piezo Systems Inc). For that, a mixture of silver glue and epoxy is used. To solidify the glue, the resulted bi-layer plate is heated inside an oven at 100 degree Celsius during one hour and then cooled down. After that, a laser machine (Siro Lasertec GmbH, Pforzheim, Germany) is used to cut each design following its CAD model. The obtained prototypes in Fig.6-(b) are then connected to wires using the same gluing process mentioned previously. Finally, a small magnet is attached to the tip of each prototype. Such magnets are useful to generate a mechanical vibration when excited by an electromagnet. It is worth noting that a rectangle domain is added on each obtained design in order to clamp the prototypes on the experimental bench support.

B. Experimental Bench

As it is shown in Fig. 6-(a), the experimental setup consists of a signal generator to produce sine voltage which is connected to an electromagnetic device that produces magnetic force to attract or pull the magnet attached at the tip of the designs. The design is clamped by a 3D printed support to completely simulate the clamped part in the modelling and COMSOL. The support itself is attached on a 3 degrees of freedom micro positioner through which it is possible to precisely determine the distance of the design to the electromagnet excitation device. The whole setup is placed on an anti-vibration table to avoid the ambient vibration that may excite the system. Finally, an oscilloscope with 4 inputs is used to measure the voltage produced by each prototype.

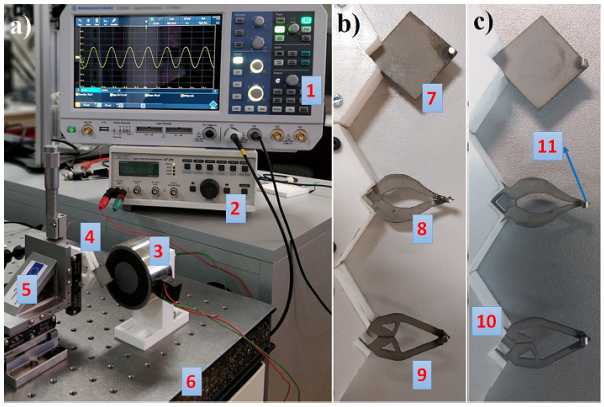

Fig. 6. a) Experimental setup, b) Fabricated designs with magnet direction (1), c) Magnet direction (2). 1: Oscilloscope, 2: Signal generator, 3: Electromagnet, 4: Design, 5: Micro positioner, 6: Anti-vibration table 7: Full plate design 8: Optimized design(1), 9: Optimized design(2), 10: 3D printed supports, 11: Glued magnets

C. Experimental Results

It should be mentioned that the full plate and design (1) have 3 electrodes while design (2) has 5 electrodes. For all designs the middle electrode is the ground electrode. In this case, the voltage of each electrode in each design is measured separately and the final reported voltage is the summation of these voltages.

In the first investigation, the magnet is put on the designs as it is shown in Fig. 6-(b). with this direction of the magnet, the force is always in the z direction or in other words, the excitation is a bending force. The sine voltage from the signal generator is set to have 10 volts amplitude and 20Hz frequency. With the help of micro positioner the design is put close to the electromagnet device and the distance is maintained for each design to guarantee the same experimental conditions. The obtained voltage for each design can be seen in Fig. 7-(a). The improvement of optimized design (1) and (2) with respect to full plate design is 1.81 and 2.17 respectively.

In the second experiment, direction of the magnet is changed based on Fig. 6-(c). With this direction, an in-plane excitation force is imposed. The obtained voltage for this new configuration is illustrated in Fig. 7-(b). For this case, the improvement of optimized design (1) and (2) with respect to full plate design is 1.005 and 1.93 respectively.

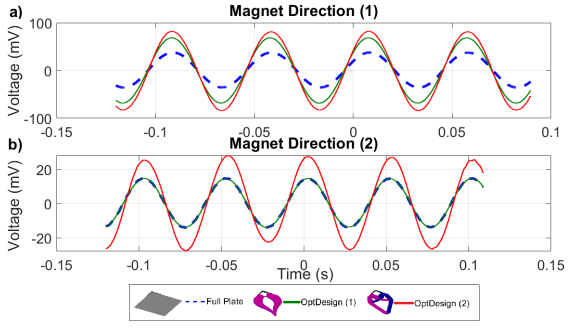

Fig. 7. Oscilloscope voltage measurements for different prototypes subjected to two direction of harmonic excitation with 20 Hz frequency

D. Discussion

The improvement of the optimized design's electrical output with respect to the full plate design in experimental setup is less than the numerical results. This can be due to laser cutting procedure which can degrade the performance of the piezoelectric material. Laser heats up the design on the edges and the material in vicinity of the edge can pass the curie temperature and act like a passive material after. This phenomenon is more severe for optimized designs which have more edges and thin parts in comparison with full plate. To overcome this problem, femtosecond lasers with higher power and less heat or diamond cutting process can be used. The other reason can be due to the neglected damping.

The COMSOL simulation results for perfectly separated electrodes based on the polarization profile shows maximum of 10 percent improvement over the current electrode placement. However, in this case more wiring is needed and it will make the electrical circuit behind more complicated and it can even increase the overall weight and volume of the design.

To improve the reliability and durability of the piezoelectric energy harvesters in the real applications, maximum applied force or displacement can be restricted by solid frames or mechanical stoppers.

Final point is that just one excitation frequency (20 Hz) is considered in the optimization. However, by increasing the excitation frequency, before reaching to vicinity of the fundamental natural frequency the results of optimization do not change.

VI. Conclusion

The structure of a piezoelectric plate is optimized by topology optimization algorithm. By relaxing the optimization procedure from numerical instabilities, polarization optimization is also augmented to the modelling and a fabrication process with its inherit challenges is proposed to fabricate the optimized designs. By eliminating the charge cancellation within each layer which was the major goal, improvement of the optimized designs over conventional full plate in harvesting the energy from random direction of excitation force is demonstrated by numerical simulation and experimental investigation. Future works in this field would consider the tuning of the resonance frequency for multiple directions.

ACKNOWLEDGMENT

Authors would like to thank Dr. Joel Agnus and Eng. Patrick Rougeot from FEMTO-ST institute for their insightful advise and help during the fabrication process.

References

[1] P. D. Mitcheson, E. M. Yeatman, G. K. Rao, A. S. Holmes, and T. C. Green, "Energy harvesting from human and machine motion for wireless electronic devices," *Proc. of the IEEE*, vol. 96(9), pp. 1457–1486, 2008.

[2] Y. Shi, Y. Wang, D. Mei, B. Feng, and Z. Chen, "Design and fabrication of wearable thermoelectric generator device for heat harvesting," *IEEE Robotics and Automation Letters*, vol. 3, no. 1, pp. 373–378, 2017.

[3] A. A. Babayo, M. H. Anisi, and I. Ali, "A review on energy management schemes in energy harvesting wireless sensor networks," *Renewable and Sustainable Energy Reviews*, vol. 76, pp. 1176–1184, 2017.

[4] V. R. Jain, R. Bagree, A. Kumar, and P. Ranjan, "wildcense: Gps based animal tracking system," in *Int Conf on Intelligent Sensors, Sensor Networks and Information Processing*, 2008, pp. 617–622.

[5] R. Salazar, G. Taylor, M. Khalid, and A. Abdelkefi, "Optimal design and energy harvesting performance of carangiform fish-like robotic system," *Smart Materials and Structures*, vol. 27, no. 7, p. 075045, 2018.

[6] S.-G. Kim, S. Priya, and I. Kanno, "Piezoelectric mems for energy harvesting," *MRS bulletin*, vol. 37, no. 11, pp. 1039–1050, 2012.

[7] J. Twiefel and H. Westermann, "Survey on broadband techniques for vibration energy harvesting," *Journal of Intelligent Material Systems and Structures*, vol. 24, no. 11, pp. 1291–1302, 2013.

[8] A. Toprak and O. Tigli, "Piezoelectric energy harvesting: State-of-the-art and challenges," *Applied Physics Reviews*, vol. 1(3), p. 031104, 2014.

[9] T. Schlinquer, A. Mohand-Ousaid, and M. Rakotondrabe, "Optimal design of a unimorph piezoelectric cantilever devoted to energy harvesting to supply animal tracking devices," *IFAC WC*, pp. 14 600–14 605, 2017.

[10] K. Rabenorosoa and M. Rakotondrabe, "Performances analysis of piezoelectric cantilever based energy harvester devoted to mesoscale intrabody robot," *SPIE Conference*, pp. 9494–28, 2015.

[11] M. Rakotondrabe, "Performances inclusion for stable interval systems," *American Control Conference*, pp. 4367–4372, 2011.

[12] S. Khadraoui, P. Lutz, and M. Rakotondrabe, "Optimal design of piezoelectric cantilevered actuators with guaranteed performances by using interval techniques," *IEEE Transactions on Mechatronics*, pp. 1660–1668, 2014.

[13] M. P. Bendsoe and O. Sigmund, *Topology Optimization Theory, Methods and Applications*. Springer Science & Business Media, 2013.

[14] M. P. Bendsøe, "Optimal shape design as a material distribution problem," *Structural optimization*, vol. 1, no. 4, pp. 193–202, 1989.

[15] M. P. Bendsøe and O. Sigmund, "Material interpolation schemes in topology optimization," *Archive of applied mechanics*, vol. 69, no. 9-10, pp. 635–654, 1999.

[16] K. Liu and A. Tovar, "An efficient 3d topology optimization code written in matlab," *Structural and Multidisciplinary Optimization*, vol. 50, no. 6, pp. 1175–1196, 2014.

[17] E. N. Silva, J. O. Fonseca, and N. Kikuchi, "Optimal design of piezoelectric microstructures," *Computational mechanics*, vol. 19, no. 5, pp. 397–410, 1997.

[18] M. Kögl and E. C. Silva, "Topology optimization of smart structures: design of piezoelectric plate and shell actuators," *Smart materials and Structures*, vol. 14, no. 2, p. 387, 2005.

[19] O. Menuzzi, J. S. Fonseca, E. A. Perondi, J. F. Gonçalves, E. Padoin, and O. A. Silveira, "Piezoelectric sensor location by the observability gramian maximization using topology optimization," *Computational and Applied Mathematics*, vol. 37, no. 1, pp. 237–252, 2018.

[20] B. Zheng, C.-J. Chang, and H. C. Gea, "Topology optimization of energy harvesting devices using piezoelectric materials," *Structural and Multidisciplinary Optimization*, vol. 38, no. 1, pp. 17–23, 2009.

[21] A. H. Amlashi, A. Mohand-Ousaid, and M. Rakotondrabe, "Topology optimization of piezoelectric plate energy harvester under external in-plan force considering different boundary conditions," in *Int Conf on Manipulation, Automation and Robotics at Small Scales*, 2019, pp. 1–6.

[22] J. Y. Noh and G. H. Yoon, "Topology optimization of piezoelectric energy harvesting devices considering static and harmonic dynamic loads," *Advances in Engineering Software*, vol. 53, pp. 45–60, 2012.

[23] R. Salas, F. Ramírez, W. Montealegre-Rubio, E. Silva, and J. Reddy, "A topology optimization formulation for transient design of multi-entry laminated piezocomposite energy harvesting devices coupled with electrical circuit," *International Journal for Numerical Methods in Engineering*, vol. 113, no. 8, pp. 1370–1410, 2018.

[24] Z. Lin, J. Chen, X. Li, J. Li, J. Liu, Q. Awais, and J. Yang, "Broadband and three-dimensional vibration energy harvesting by a non-linear magnetoelectric generator," *Applied Physics Letters*, vol. 109, no. 25, p. 253903, 2016.

[25] D. V. Hutton and J. Wu, *Fundamentals of finite element analysis*. McGraw-hill New York, 2004, vol. 1.

[26] R. Lerch, "Simulation of piezoelectric devices by two-and three-dimensional finite elements," *IEEE transactions on ultrasonics, ferroelectrics, and frequency control*, vol. 37, no. 3, pp. 233–247, 1990.

[27] B. V. de Almeida, D. C. Cunha, and R. Pavanello, "Topology optimization of bimorph piezoelectric energy harvesters considering variable electrode location," *Smart Materials and Structures*, 2019.

[28] K. Svanberg, "The method of moving asymptotes—a new method for structural optimization," *International journal for numerical methods in engineering*, vol. 24, no. 2, pp. 359–373, 1987.

[29] T. Schlinquer, A. Mohand-Ousaid, and M. Rakotondrabe, "Displacement amplifier mechanism for piezoelectric actuators design using simp topology optimization approach," in *IEEE ICRA*, 2018, pp. 1–7.